

Dynamic Jahn-Teller effect in electron transport through single C_{60} molecules

T. Frederiksen,^{1,2,*} K. J. Franke,³ A. Arnau,^{1,4,5} G. Schulze,³ J. I. Pascual,³ and N. Lorente⁶

¹*Donostia International Physics Center (DIPC), Manuel de Landizabal Pasealekua 4, E-20018 Donostia-San Sebastián, Spain*

²*CIC nanoGUNE Consolider, Mikeletegi Pasealekua 56, E-20009 Donostia-San Sebastián, Spain*

³*Institut für Experimentalphysik, Freie Universität Berlin, Arnimallee 14, D-14195 Berlin, Germany*

⁴*Depto. de Física de Materiales UPV/EHU, Facultad de Química, Apartado 1072, E-20080 Donostia-San Sebastián, Spain*

⁵*Centro de Física de Materiales, Centro Mixto CSIC-UPV/EHU, E-20080 Donostia-San Sebastián, Spain*

⁶*Centre d'Investigació en Nanociència i Nanotecnologia (CSIC-ICN),
Campus de la Universitat Autònoma de Barcelona, E-08193 Bellaterra, Spain*

(Dated: April 21, 2008)

Scanning tunneling spectra on single C_{60} molecules that are sufficiently decoupled from the substrate exhibit a characteristic fine structure, which is explained as due to the dynamic Jahn-Teller effect. Using electron-phonon couplings extracted from density functional theory we calculate the tunneling spectrum through the C_{60}^- anionic state and find excellent agreement with measured data.

PACS numbers: 73.63.-b, 68.37.Ef, 63.22.-m, 71.70.Ej

Orbital electronic degeneracy and stability of the nuclear configuration are incompatible unless the atoms of a molecule lie on a straight line. This statement is due to Jahn and Teller [1], who proved its general validity in 1937 using group theory [2]. The theorem has important implications for non-linear molecules with a degenerate electronic ground state, particularly when the degenerate electrons participate in the binding of the molecule. In such cases the molecule undergoes a structural distortion which lifts the electronic degeneracy by reducing the symmetry of the nuclear configuration, known as the static Jahn-Teller (JT) effect. In certain situations *several* distortions can lower the symmetry of the molecule, and hence lift the electronic degeneracy. When such distorted states are also degenerate, the system will fluctuate between these equivalent configurations by quantum tunneling, resulting in pseudorotations [3] and restoration of the parent symmetry, denoted the dynamic JT effect [4, 5].

The buckminsterfullerene C_{60} is an exceptionally symmetric molecule, and its symmetry governs many of its physical and chemical properties. In group theory it is classified by the icosahedral point group I_h , the group with the highest number of symmetry operations in three dimensions [4]. The geometrical symmetry is also reflected in the electronic and vibrational properties, which are both highly degenerate. For instance, the highest occupied molecular orbital (HOMO) and the lowest unoccupied molecular orbital (LUMO) are orbitally fivefold and threefold degenerate, respectively. By adding electrons or holes to C_{60} these degeneracies are explored and, hence, JT physics is expected to play an important rôle [6].

Indeed, the JT effect has been reported in photoemission (PE) spectra of C_{60} in the gas phase for different charge states of the molecule [7, 8, 9, 10, 11]. Here, a fine structure in the intensity spectrum has been explained as originating in the underlying electron-phonon

(e-ph) coupled problem. Signatures of JT have also been found in luminescence spectra of C_{60} nanocrystals [12]. A more direct consequence of the JT effect has been observed in low-temperature scanning tunneling microscopy (STM) images of potassium-doped fullerenes (K_3C_{60}) on Au(111), revealing a significant static deformation of the molecular structure [13]. While vibronic effects have also been studied in the transport properties of C_{60} molecules [14, 15, 16], the dynamic JT effect in single-molecule conductance has not been reported so far, presumably due to the difficulty of decoupling a molecule sufficiently from its environment.

From the theoretical side there has been a substantial interest in describing the e-ph coupled problem in C_{60} , primarily motivated by the discovery of the superconducting phase of alkali doped fullerenes A_3C_{60} and its relation to the “conventional” e-ph mechanism [17, 18, 19]. An accurate calculation of the e-ph coupling constants is fundamental to such descriptions. In comparison with couplings fitted to photoemission data on C_{60}^- , it has been argued that couplings derived from density functional theory (DFT) are too weak [7]. Contrary, DFT couplings were later shown to accurately account for photoemission data on C_{60}^+ [10]. This apparent controversy calls for complementary studies of the e-ph interaction that put DFT-derived couplings to test.

In this Letter, we report on the JT fingerprint in the conductance spectra of single C_{60} molecules in a tunneling junction. Fullerenes were decoupled from a Au(111) surface by a template of organic molecules. Scanning tunneling spectroscopy reveals a broad sideband above a sharp LUMO-derived resonance. To understand this we calculate the tunneling spectrum by solving the JT problem from first principles. The vibrational modes, frequencies, and e-ph couplings are derived from DFT, and the excitation spectrum of the *vibronic* ground state is computed numerically by nonequilibrium Green’s function (NEGF) techniques as well as by exact diagonaliza-

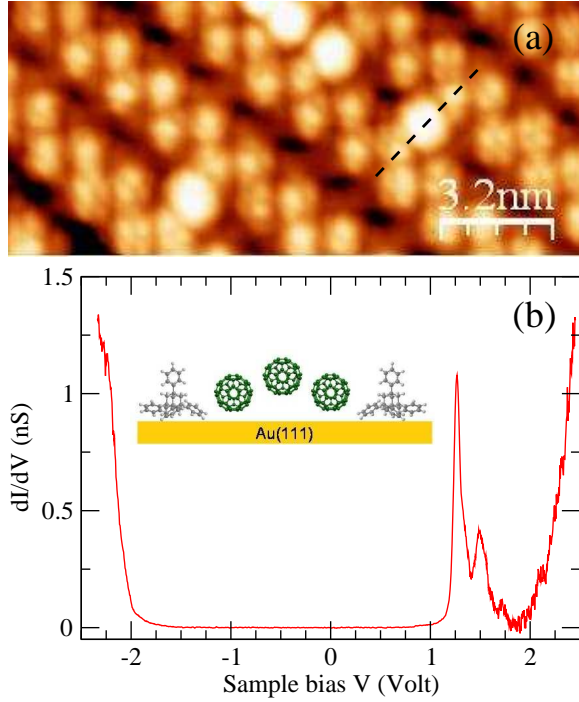


FIG. 1: (color online) (a) STM image of the double rows of alternating TPA/C₆₀ on Au(111) ($I = 16$ pA, $V = 580$ mV, $T = 5$ K). Some isolated C₆₀ molecules are adsorbed in the troughs between the rows. (b) Side view of the structural model along the dashed line in (a) and dI/dV spectra recorded on top of such a fullerene ($I_{\text{set}} = 0.46$ nA, $V_{\text{set}} = 2.5$ V, $V_{\text{rms}} = 14$ mV).

tion. The theoretical results explain the origin of the experimentally observed fine structure as due to the dynamic JT effect.

The electronic decoupling of the molecule from its metallic substrate is crucial for studying any JT-induced fine structure of the molecular resonances. To reduce this interaction experimentally we use a novel strategy based on codeposition of C₆₀ and 1,3,5,7-tetraphenyladamantane (TPA) on Au(111), which results in spontaneous formation of nanostructures where the C₆₀ cages are lifted away from the surface by support from TPA molecules [22, 23]. One of the observed structural motifs are double rows of alternating TPA and C₆₀, cf. Fig. 1(a). This dielectric template yields troughs for single C₆₀ molecules to be trapped between neighboring double rows as sketched in Fig. 1(b). Differential conductance ($dI/dV - V$) spectra taken over the center of these molecules reveal strong non-linearities around -2.2 V, 1.3 V and 2.5 V, associated with the HOMO, LUMO and LUMO+1 derived resonances, respectively (Fig. 1(b)). The corresponding large gap of ~ 3.5 eV is a clear sign of a weakly interacting molecule with its surrounding [23]. Even more striking is the observation of a very sharp LUMO-derived resonance (FWHM ~ 60 meV), reflecting a long lifetime in the order of 10 fs of the

Mode	$\hbar\omega_\nu$	$\lambda_\nu/N(0)$	Mode	$\hbar\omega_\nu$	$\lambda_\nu/N(0)$
ν	meV (cm ⁻¹)	meV	ν	meV (cm ⁻¹)	meV
$H_g(8)$	195 (1572)	14.6	$H_g(4)$	95 (766)	4.0
$A_g(2)$	185 (1491)	7.3	$H_g(3)$	86 (693)	10.2
$H_g(7)$	178 (1439)	15.0	$A_g(1)$	60 (484)	1.0
$H_g(6)$	155 (1251)	3.2	$H_g(2)$	52 (419)	11.6
$H_g(5)$	136 (1094)	4.3	$H_g(1)$	32 (256)	4.7

TABLE I: Partial electron-phonon coupling constants $\lambda_\nu/N(0) = 2/9 \sum_{i,j} |M_{i,j}^\nu|^2 / \hbar\omega_\nu$ of the A_g and H_g intramolecular modes for C₆₀, c.f. Eq. (10) of Ref. [18], with $N(0)$ being the density of states. The sum of all modes gives a coupling strength of $\lambda^{\text{GGA}}/N(0) = 76.1$ meV [26] in good agreement with previous calculations [18, 19, 20, 21].

tunneling electron. Hence, this system is ideal to study e-ph couplings. However, instead of single vibronic peaks [16], we observe a broad sideband at ~ 230 meV above the LUMO energy, which lies well outside of the 200-meV-wide vibrational spectrum of C₆₀.

Tunneling electrons through an isolated C₆₀ molecule will probe the excitation spectrum as resulting from a dynamic JT interaction with the vibrations. Near the LUMO-derived resonances in focus here, we exclude the HOMO and LUMO+1 states from our treatment since these are well separated in energy. Further, group theory gives that only the A_g and H_g intramolecular phonons couple to the t_{1u} LUMO states [6]. Thus, the JT problem for C₆₀⁻ is described by the following Hamiltonian

$$H = \varepsilon_0 \sum_{i=1}^3 c_i^\dagger c_i + \sum_{\nu=1}^{42} \hbar\omega_\nu b_\nu^\dagger b_\nu + \sum_{\nu=1}^{42} \sum_{i=1}^3 \sum_{j=1}^3 M_{i,j}^\nu c_i^\dagger c_j (b_\nu^\dagger + b_\nu), \quad (1)$$

where c_i^\dagger (c_i) is the one-electron creation (annihilation) operator corresponding to one of the three degenerate single-particle LUMO states $|i\rangle$ and b_ν^\dagger (b_ν) is the bosonic creation (annihilation) operator of each of the 42 (8 five-fold degenerate H_g and 2 non-degenerate A_g) vibrational modes ν . The parameters ε_0 , ω_ν , and $M_{i,j}^\nu$ represent the bare LUMO energy, the vibrational frequency of mode ν , and the coupling constant for the scattering of an electron from state $|i\rangle$ to state $|j\rangle$ under creation or annihilation of a phonon in mode ν , respectively. These parameters (see Tab. I) are obtained from DFT calculations [24, 25, 26] applying the scheme described in Ref. [27] to the neutral [21], isolated C₆₀ molecule.

In our STM configuration the molecule under investigation is much less coupled to the tip than to the substrate, i.e., $\Gamma_t \ll \Gamma_s$ in terms of the tip Γ_t and substrate Γ_s tunneling rates. Under this condition the electron occupancy of the molecular states is effectively in equilibrium with the substrate and the differential conductance

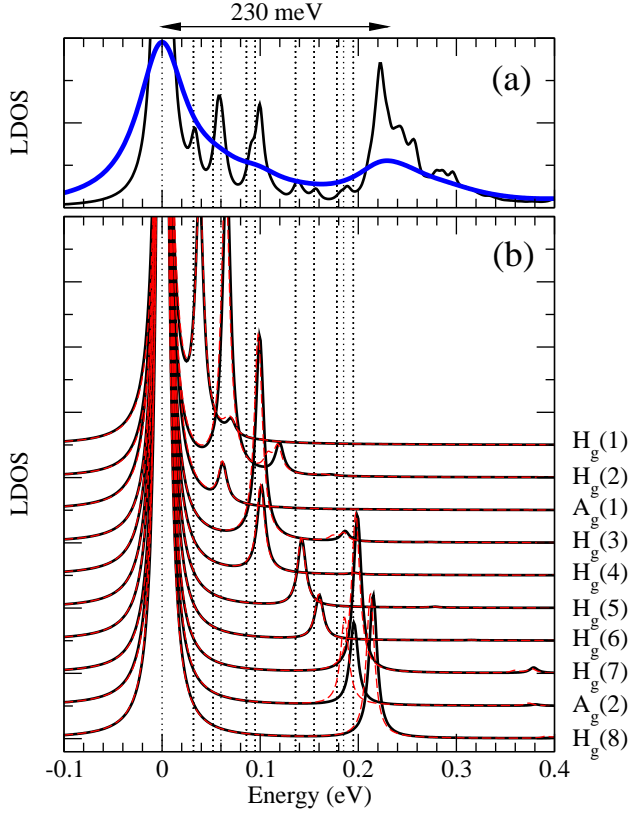


FIG. 2: (color online). (a) Theoretically computed JT-induced fine structure in the LDOS of the LUMO via the coupling to A_g and H_g modes, shown for two different intrinsic level broadenings: $\Gamma = 10$ meV (black line) and $\Gamma = 60$ meV (thick blue line). (b) Analysis of the position of the phonon sidebands including only one mode at the same time, calculated with both the SCBA (black lines) and LS (dashed red lines) methods ($\Gamma = 10$ meV). For clarity the spectra are off-set and shifted to place the main peak at zero energy. The vertical dotted lines indicate the fundamental frequencies of the A_g and H_g modes.

at a bias voltage V_s is to a first approximation proportional to $\rho(\mu_s + eV_s)\Gamma_t$, where ρ is the local density of states (LDOS). This takes into account both couplings to the leads as well as to the vibrations. We have considered two different methods for calculating ρ , namely exact diagonalization with the Lanczos scheme (LS) as well as NEGF within the self-consistent Born approximation (SCBA) [28].

Figure 2(a) shows the computed JT spectrum from SCBA for two different values of the total electronic broadening $\Gamma = \Gamma_t + \Gamma_s \approx \Gamma_s$ (FWHM). The spectrum is composed of a main peak followed by a series of sidebands at higher excitation energies. Depending on the broadening, the LUMO spectrum might appear as one main peak with a single sideband separated by 230 meV. A similar structure has also been reported in photoemission [7, 8, 9, 10]. It is important to realize that the fine structure in the LDOS does not relate in a simple way to

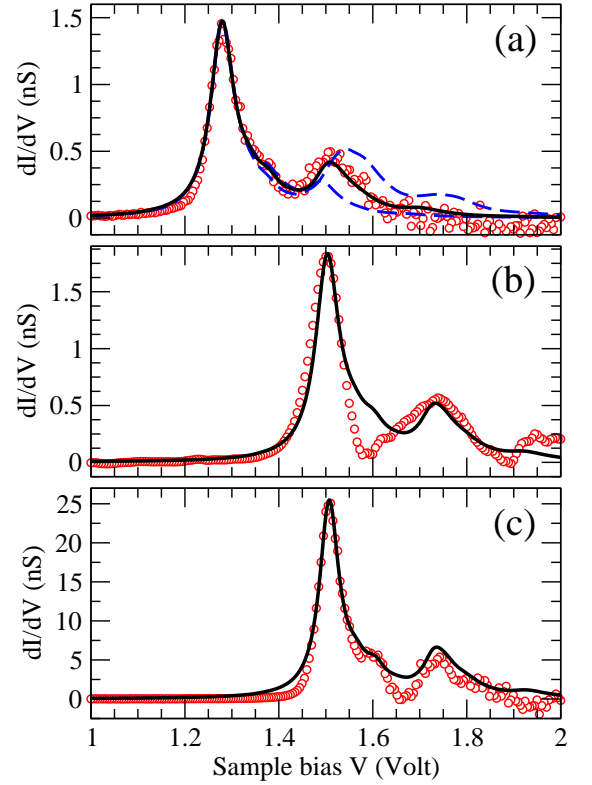


FIG. 3: (color online). Direct comparison between experiment (red circles) and theory (black line) for three different molecules: (a) $I_{\text{set}} = 0.3$ nA, $V_{\text{set}} = 2.5$ V, $V_{\text{rms}} = 7$ mV, $\Gamma_s = 60$ meV. (b) $I_{\text{set}} = 0.52$ nA, $V_{\text{set}} = 2.5$ V, $V_{\text{rms}} = 3.5$ mV, $\Gamma_s = 60$ meV. (c) $I_{\text{set}} = 1.2$ nA, $V_{\text{set}} = 2.5$ V, $V_{\text{rms}} = 7$ mV, $\Gamma_s = 50$ meV. Panel (a) includes calculations with scaled e-ph coupling constants (dashed blue lines) corresponding to $\lambda_\nu \rightarrow 1/2 \lambda_\nu^{\text{GGA}}$ and $\lambda_\nu \rightarrow 2 \lambda_\nu^{\text{GGA}}$.

the fundamental frequencies of the A_g and H_g modes (in the range 32-195 meV as indicated with vertical dotted lines in Fig. 2). Hence, for JT systems it is not possible to directly relate vibronic structure in spectroscopy with molecular frequencies. Another important fact is that the vibronic spectrum is threefold degenerate, i.e., the parent symmetry of the LUMO is restored by the A_g and H_g modes as expected from the *dynamic* JT effect [29]. Hence, the molecule is not statically distorted.

To gain an understanding of the contributions from the different vibrational modes to the total spectrum, we show in Fig. 2(b) the LDOS as resulting from a calculation with the coupling to only one type of mode at a time. Although the sideband structure is much simpler, one observes that the peak separation for all H_g modes is larger than the phonon energy. This nontrivial behavior is generic to the $T_{1u} \otimes h_g$ JT problem [6]. Figure 2(b) also shows that, except for the more strongly coupled $A_g(2)$ mode, SCBA and LS yield essentially the same results for the LDOS due to the weak e-ph couplings.

We next turn to a comparison with the experiment.

The measured tunneling spectra on different molecules exhibit certain variations in peak position and structure around the LUMO resonance. This variation is likely due to slightly different environments, and possibly also molecular orientation, of the selected C_{60} species. In Fig. 3 we compare the dI/dV -spectra of three different molecules with theoretical spectra by applying an appropriate substrate coupling Γ . The relative peak height as well as the position of the sideband with respect to the main peak are in very good agreement. This fact supports the interpretation that these spectra indeed exhibit the free-molecule JT effect.

Alternative mechanisms, such as the weak spin-orbit coupling in carbon [4] or the Stark effect from the applied voltage, cannot account for the 230 meV splitting seen in Fig. 3. Although details in the weak electronic coupling of the C_{60} molecule to its environment may have an influence in the experimentally recorded spectra, we believe that this effect solely cannot produce such an agreement as the JT theory presented above for a decoupled molecule. Furthermore, from the different timescales of electron tunneling events and residence times in the molecule, we can also exclude heating effects. Based on the NEGF-SCBA calculations we find that heating would be important if the current through the LUMO states is raised by two orders of magnitude.

In Fig. 3(a) we also show how the calculated spectrum changes by a scaling of the DFT-derived e-ph couplings corresponding to $\lambda_\nu \rightarrow 1/2 \lambda_\nu^{\text{GGA}}$ and $\lambda_\nu \rightarrow 2 \lambda_\nu^{\text{GGA}}$. As seen, these scalings decimate the agreement with experiment in terms of peak ratio and separation, thus pointing towards reasonable values of the e-ph coupling strength within DFT.

In summary, we have explained the dynamic JT effect as it is revealed in electron tunneling spectroscopy through the C_{60}^- anionic state of sufficiently isolated molecules. The experimental realization of this situation was based on a novel experimental preparation procedure of codeposition of C_{60} and TPA molecules on Au(111), where C_{60} molecules on top of the double row template are exceptionally decoupled, geometrically and electronically, from the metallic substrate. Low-temperature STM dI/dV spectra recorded under such conditions display a delicate fine structure around the LUMO-derived resonance, that closely resembles the theoretically computed JT spectrum. This quantitative agreement further supports that the calculated e-ph couplings from DFT provide an accurate description for the vibrational interactions in the molecule.

TF acknowledges support from the Danish FNU (grant 272-07-0114). AA and TF thank partial financial support from UPV/EHU (grant IT-366-07) and MEC (grant FIS2007-66711-C02-01). NL acknowledges support from MEC (grant FIS2006-12117-C04-01). Financial support by the DFG through SPP 1243 and Sfb 658 is gratefully acknowledged. We thank S. Zarwell and K. Rück-Braun

for the synthesis of the TPA molecules. JIP and KJF acknowledge fruitful discussions with F. von Oppen.

* Electronic address: thomas.frederiksen@ehu.es

- [1] H. A. Jahn and E. Teller, Proc. R. Soc. London Ser. A **161**, 220 (1937).
- [2] The only exception being “accidental” degeneracy, i.e., when the electronic degeneracy not caused by symmetry.
- [3] I. D. Hands, J. L. Dunn, and C. A. Bates, Phys. Rev. B **73**, 235425 (2006).
- [4] M. S. Dresselhaus, G. Dresselhaus, and P. C. Eklund, *Science of Fullerenes and Carbon Nanotubes*, Academic Press, 1995.
- [5] W.-Z. Wang, A. R. Bishop, L. Yu, Phys. Rev. B **50**, 5016 (1994).
- [6] N. Manini, E. Tosatti, A. Auerbach, Phys. Rev. B **49**, 13008 (1994); O. Gunnarsson *ibid.* **51**, 3493 (1995); J. L. Dunn and C. A. Bates, *ibid.* **52**, 5996 (1995).
- [7] O. Gunnarsson *et al.*, Phys. Rev. Lett. **74**, 1875 (1995).
- [8] P. A. Brühwiler *et al.*, Chem. Phys. Lett. **279**, 85 (1997).
- [9] S. E. Canton *et al.*, Phys. Rev. Lett. **89**, 045502 (2002); N. Manini, E. Tosatti, *ibid.* **90**, 249601 (2003); S. E. Canton *et al.*, *ibid.* **90**, 249602 (2003).
- [10] N. Manini, P. Gattari, and E. Tosatti, Phys. Rev. Lett. **91**, 196402 (2003).
- [11] S. Tomita, *et al.*, Phys. Rev. Lett. **94**, 053002 (2005).
- [12] E. Čavar *et al.*, Phys. Rev. Lett. **95**, 196102 (2005).
- [13] A. Wachowiak *et al.*, Science **310**, 468 (2005).
- [14] H. Park *et al.*, Nature **407**, 57 (2000).
- [15] J. I. Pascual *et al.*, J. Chem. Phys. **117**, 9531 (2002).
- [16] N. A. Pradhan, N. Liu, and W. Ho, J. Phys. Chem. B **109**, 8513 (2005).
- [17] C. M. Varma, J. Zaanen, and K. Raghavachari, Science **254**, 989 (1991).
- [18] V. P. Antropov, O. Gunnarsson, and A. I. Liechtenstein, Phys. Rev. B **48**, 7651 (1993).
- [19] O. Gunnarsson, Rev. Mod. Phys. **69**, 575 (1997).
- [20] N. Manini *et al.*, Philos. Mag. B **81**, 793 (2001).
- [21] M. Saito, Phys. Rev. B **65**, 220508(R) (2002).
- [22] K. J. Franke *et al.*, Phys. Rev. Lett. **100**, 036807 (2008).
- [23] I. Fernández-Torrente, K. J. Franke, and J. I. Pascual, J. Phys.: Condens. Matter, **20**, 184001 (2008).
- [24] We use the SIESTA implementation of DFT [25] with an optimized double- ζ plus polarization basis set for the valence electrons, the generalized gradient approximation (GGA-PBE) for exchange-correlation, a relativistic Troullier-Martins pseudopotential for the core electrons, and a 200 Ry cutoff for real-space grid integrations.
- [25] J. M. Soler *et al.*, J. Phys.: Condens. Matter **14**, 2745 (2002).
- [26] The local density approximation (LDA) leads to a similar coupling strength $\lambda^{\text{LDA}}/N(0) = 74.2$ meV, but vibrational frequencies are generally overestimated.
- [27] T. Frederiksen, M. Paulsson, M. Brandbyge, and A.-P. Jauho, Phys. Rev. B **75**, 205413 (2007).
- [28] The polaronic Hartree diagram is neglected.
- [29] As expected from the JT theorem, the electronic degeneracy is broken if the symmetry of the e-ph couplings are disturbed, e.g., by coupling only to one of the five H_g (8) modes.